View metadata, citation and similar papers at core.ac.uk

brought to you by CORE

provided by Elsevier - Publisher Connector

Available online at www.sciencedirect.com

SCIENCE DIRECT

ELSEVIER

Genomics 86 (2005) 731 – 738

GENOMICS

www.elsevier.com/locate/ygeno

A 12,000-rad porcine radiation hybrid (IMNpRH2) panel refines the conserved synteny between SSC12 and HSA17

Wan-Sheng Liu [a,*], Katie Eyer [a], Hiroshi Yasue [b], Benjamin Roelofs [a], Hideki Hiraiwa [b], Takeshi Shimogiri [c], Earl Landrito [a], Joseph Ekstrand [a], Michael Treat [a], Anette Rink [d], Martine Yerle [e], Denis Milan [e], Craig W. Beattie [a]

[a] *Department of Animal Biotechnology, College of Agriculture, Biotechnology, and Natural Resources, University of Nevada at Reno, Mail Stop 202, 1664 N. Virginia Street, Reno, NV 89557, USA*

[b] *Genome Research Department, National Institute of Agrobiological Sciences, Ikenodai, Tsukuba, Ibaraki 305-0901, Japan*

[c] *Faculty of Agriculture, Kagoshima University, Korimoto, Kagoshima 890-0065, Japan*

[d] *Animal Disease and Food Safety Laboratory, Department of Agriculture, State of Nevada, Reno, NV, USA*

[e] *Laboratoire de Génétique Cellulaire, Institut National de la Recherche Agronomique, BP27, 31326 Castenet-Tolosan Cedex, France*

Received 7 April 2005; accepted 8 August 2005
Available online 11 November 2005

Abstract

Reverse or bidirectional Zoo-FISH suggests that synteny between porcine chromosome 12 (SSC12) and human chromosome 17 (HSA17) is completely conserved. The construction of a high-resolution radiation hybrid (RH) map for SSC12 provides a unique opportunity to determine whether chromosomal synteny is reflected at the molecular level by comparative gene mapping of SSC12 and HSA17. We report an initial, high-resolution RH map of SSC12 on the 12,000-rad IMNpRH2 panel using CarthaGene software. This map contains a total of 320 markers, including 20 microsatellites and 300 ESTs/genes, covering ~4836.9 $cR_{12,000}$. The markers were ordered in 16 linkage groups at LOD 6.0 using framework markers previously mapped on the $IMpRH_{7000\text{-}rad}$ SSC12 and porcine genetic maps. Ten linkage groups ordered more than 10 markers, with the largest containing 101 STSs. The resolution of the current RH map is ~15.3 kb/cR on SSC12, a significant improvement over the second-generation EST SSC12 $RH_{7000\text{-}rad}$ map of 103 ESTs and 15 framework markers covering ~2287.2 cR_{7000}. Compared to HSA17, six distinct segments were identified, revealing macro-rearrangements within the apparently complete synteny between SSC12 and HSA17. Further analysis of the order of 245 genes (ESTs) on HSA17 and SSC12 also revealed several micro-rearrangements within a synteny segment. A high-resolution SSC12 $RH_{12,000\text{-}rad}$ map will be useful in fine-mapping QTL and as a scaffold for sequencing this chromosome.
© 2005 Elsevier Inc. All rights reserved.

Keywords: Radiation hybrid map; Comparative map; SSC12; HSA17; Microsatellite; EST; Swine

Introduction

Radiation hybrid (RH) mapping is based on analysis of the marker distribution among a panel of host cell lines containing random genomic fragments of a target genome [1]. This mapping approach has advantages over other methods: it does not require markers to be polymorphic, map resolution is controlled by simply changing the radiation dose, and it is a faster and relatively inexpensive way to construct a high-resolution physical map. RH mapping has become the most popular and efficient method of building physical maps for several domestic animal species, including pigs. To date, four different RH panels have been reported for swine: a 3000-rad panel (T43RH; Research Genetics, Huntsville, AL, USA) used for constructing maps of porcine chromosomes 2 (SSC2), 6, and X [2–4]; a 5000-rad panel (SSRH) [5] used for a whole-genome (WG) EST map [6]; a 7000-rad panel (IMpRH) [7,8] used widely to create chromosomal and WG–RH maps [9–15]; and a 12,000-rad panel (IMNpRH2) [16] for high-resolution mapping in a chromosomal region of interest in swine [17,18] and a scaffold for sequencing the swine genome.

The priority for constructing an initial RH map for SSC12 was twofold. First, reverse or bidirectional Zoo–fluorescence

* Corresponding author. Fax: +1 775 784 1375.
E-mail address: wsliu@cabnr.unr.edu (W.-S. Liu).

0888-7543/$ - see front matter © 2005 Elsevier Inc. All rights reserved.
doi:10.1016/j.ygeno.2005.08.006

in situ hybridization (FISH) suggests that synteny between SSC12 and human chromosome 17 (HSA17) is highly conserved [19–21]. This provides a unique opportunity to use gene sequences on HSA17 to increase marker density on SSC12 and determine whether chromosomal synteny is reflected at the molecular level by comparative mapping. Second, SSC12 harbors at least 12 reported quantitative trait loci (QTL) associated with growth [22–25], meat quality [26–30], reproduction [31,32], and immune capacity [33].

SSC12 has been analyzed by linkage analysis [34–36], somatic hybrid cell mapping [37], RH mapping [5,6,8,11,15,38–40], and comparative gene mapping [41,42]. Approximately 35 genes and ESTs have been mapped on the SSC12 cytogenetic map (http://www.toulouse.inra.fr/lgc/pig/cyto/genmar/htm/12GM.HTM, last updated 2002) and 28 microsatellites (http://www.marc.usda.gov/genome/genome.html) on the SSC12 linkage map, resulting in a low-density map for the chromosome. Although our first-generation porcine EST $RH_{7000\text{-}rad}$ map containing 51 ESTs (genes) on SSC12 [11] has been published and improved recently by doubling the marker number (118) on a second-generation EST RH map (http://www.ag.unr.edu/beattie/research/second_generation.htm, Rink et al., submitted for publication), the current 7000-rad RH map of SSC12 still lacks the resolution required for either fine-mapping of the reported QTL or firmly establishing the degree of conservation between SSC12 and HSA17. We used HSA17 and the IMNpRH2 panel to develop a high-resolution comprehensive map of SSC12. The resulting SSC12 $RH_{12,000\text{-}rad}$ map contains 320 markers including 20 framework microsatellites (MSs) and 300 ESTs/genes, covering ~4836.9 $cR_{12,000}$.

Results

SSC12 $RH_{12,000\text{-}rad}$ map

Initially, a total of 337 markers (Supplementary Table 1) were typed on the 12,000-rad IMNpRH2 panel, and marker order was determined using CarthaGene software [43,44]. At LOD 6.0, 16 linkage groups (L1 to L16) (Fig. 1) were identified with 17 singletons (6 genes, 5 ESTs, and 6 MSs). Ten of these linkage groups contained more than 10 markers, with the largest (L6 in Fig. 1) having 101 STSs. Four linkage groups (L2, L6, L10, and L15) were anchored on the cytogenetic map (http://www.toulouse.inra.fr/lgc/pig/cyto/genmar/htm/12GM.HTM) and 6 linkage groups (L2, L6, L9, L10, L12, and L13) on the genetic map (http://www.marc.usda.gov/genome/genome.html) based on the common markers on the maps. The order and orientation of the linkage groups were determined based on markers mapped on the SSC12 genetic map (http://www.marc.usda.gov/genome/genome.html) and the ESTs/genes ordered on the first- [11] and second-generation EST $RH_{7000\text{-}rad}$ maps (http://www.ag.unr.edu/beattie/research.htm). This initial SSC12 $RH_{12,000\text{-}rad}$ map contains 320 markers including 20 MSs, 202 genes, and 98 ESTs, covering ~4836.9 cR. In 4 instances there were 3 ESTs/genes [*H3F3B–ITGB4–GALK1* (L2 in Fig. 1), *PSME3–AR043A10–PRKWNK4* (L6), and *AR056G04–ACADVL–HSA011916* and *MPDU1–FXR2–EIF4A1* (L13)] with an identical RH vector. These were assigned to the same map position. In 18 other cases, 2 ESTs/genes [*FASC–RACS3* (L1), *AR058H05–AR050A05* (L5), *LOC51629–RPIP8, AR025H09–ITGA2B, AR029G01–UNR6203C07, CNTNAP1–EZH1, RAB5C–GCN5L2, MGC9753–MLN64, AR094D04–AR072C03, AR012H09–NDP52* and *FLJ21347–FLJ11164* (L6), *FLJ20739–MRPS23* and *MKP–AP1GBP1* (L9), *CTNS–CARKL* (L11), *DDX33–MGC4189* and *ENO3–SE259162* (L13), and *SCO1–PMP22* and *LLGL1–TOP3A* (L16)] mapped to the same map position (Fig. 1), for a total of 294 effective map positions in the SSC12 $RH_{12,000\text{-}rad}$ map. As the size of SSC12 was estimated at 74 Mb [45], slightly smaller than HSA17 [~78 Mb (Fig. 2), http://www.ncbi.nlm.nih.gov/mapview/maps.cgi?taxid=9606&chr=17], the resolution of the SSC12 $RH_{12,000\text{-}rad}$ map is ~15.3 kb/$cR_{12,000}$. Compared to the second-generation SSC12 EST $RH_{7000\text{-}rad}$ map (http://www.ag.unr.edu/beattie/research.htm), with 103 ESTs and 15 framework markers covering 2287 cR_{7000} (~34 kb/cR_{7000}), the current resolution of the SSC12 $RH_{12,000\text{-}rad}$ map is twofold (34/15.3 = 2.2) higher than that of the $RH_{7000\text{-}rad}$ map.

The retention frequency (RF) of the 337 SSC12 markers ranged from 7.8 (*TP53*) to 50.0% (*ATP5G1*); the average was 32.1% (Supplementary Table 1). This average is slightly lower than the estimated frequency of 35.4% reported for the entire genome in the IMNpRH2 panel [16]. When analyzing the RF of markers along the map, we noticed three interesting regions. The first region is located on SSC12q between *ALOX12* (L13 in Fig. 1) and *P101-P13K* (L14), containing 20 markers that all had a significantly lower RF, ranging from 7.8 to 24.4% with an average of 16.4% (Supplementary Table 1). Of 337 markers typed on the IMNpRH2 panel, 8 were identified to have a RF <15.0%. All of these lower RF markers were located in this region. The second region corresponds to the centromere of SSC12 between *AR054D02* (L6) and *MGC15396* (L6), which contains 19 markers with an average RF of 39.1%. The third region contains another 19 markers located on SSC12q between *S0147* (L9) and *TIAF1* (L10) with an average RF of 44.7%. Human orthologs in this region are all localized between 23 and 30 Mb on HSA17, where the centromere of HSA17 is located (Fig. 1).

As described under Materials and methods, two markers (one made in Japan, the other in the United States) for nine genes, *AP2B1, GRB2, LOC81558, NDP52, RPA1, SCAP1, SMARCE1, STAT5A*, and *TOP2A*, were typed separately on the IMNpRH2 panel. In the case of *NDP52*, the two markers mapped to the same position. For the remaining eight genes, the paired markers mapped next to each other within a narrow interval of 8.2 $cR_{12,000}$ (range 2.5 to 12.8 $cR_{12,000}$) (Fig. 1). The physical distances (in kilobases) between the paired markers could not be determined, as the porcine genome sequence is not available. However, by comparing the sequences of the PCR fragments amplified using primer pairs against the human

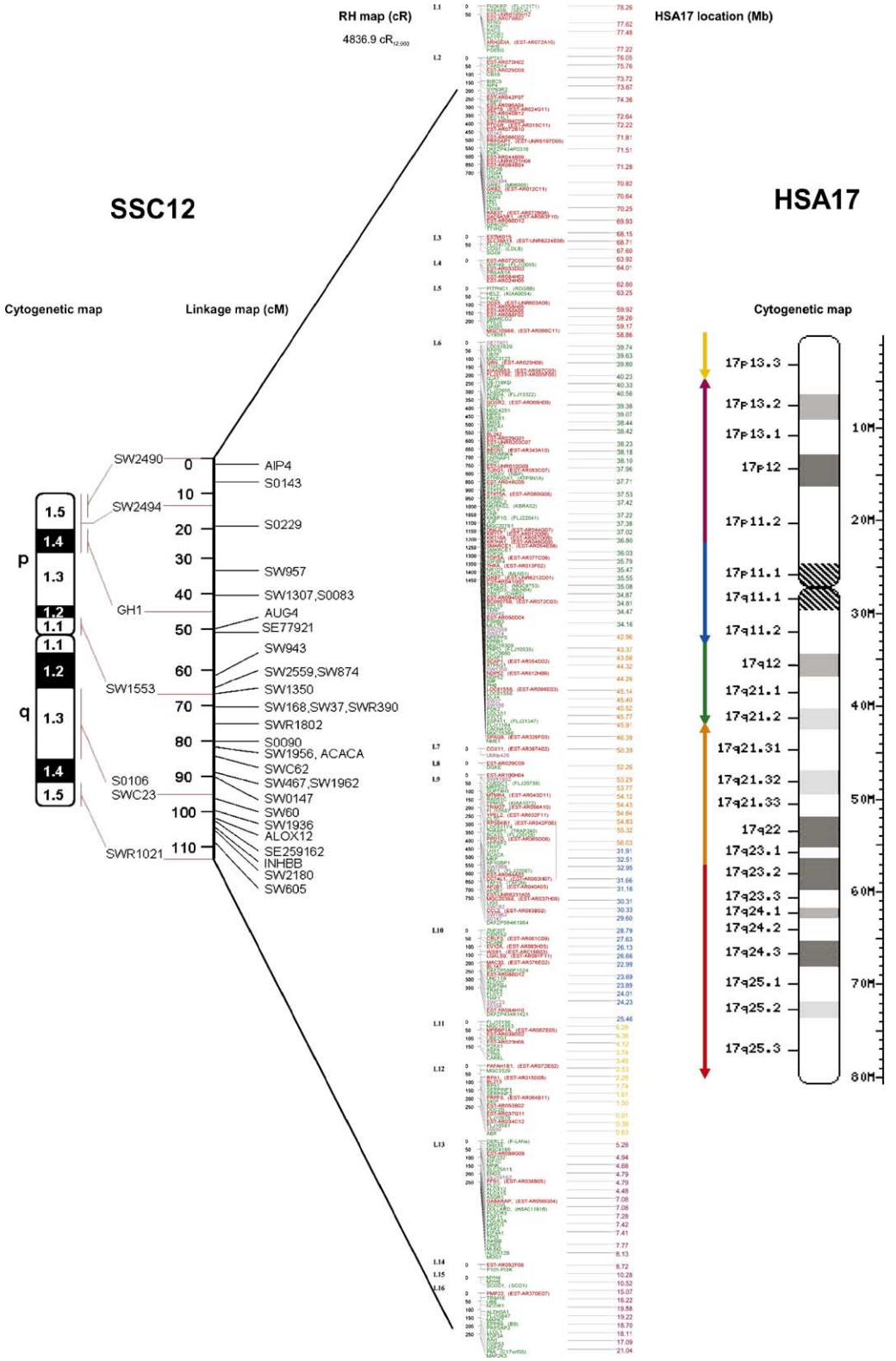

Fig. 1. A high-resolution $RH_{12,000\text{-rad}}$ map for SSC12 compared with HSA17. A total of 320 markers including 20 microsatellites (purple), 202 genes (green), and 98 ESTs (red) in 16 linkage groups (L1–L16) are ordered at LOD 6.0. The order and orientation of the linkage groups were determined based on the markers mapped on the SSC12 linkage map and the ESTs/genes ordered in the $RH_{7000\text{-rad}}$ maps. On the left of the RH map are the cytogenetic and linkage maps of SSC12. On the right of the RH map are the gene locations on HSA17 and the HSA17 cytogenetic map. The colored arrows on the left of HSA17 indicate the orientation of synteny groups of genes on the SSC12 RH map. The scale on the right of HSA17 indicates the positions of the sequence in megabases. The rearrangement of genes in the box (L9) is discussed in detail in the text.

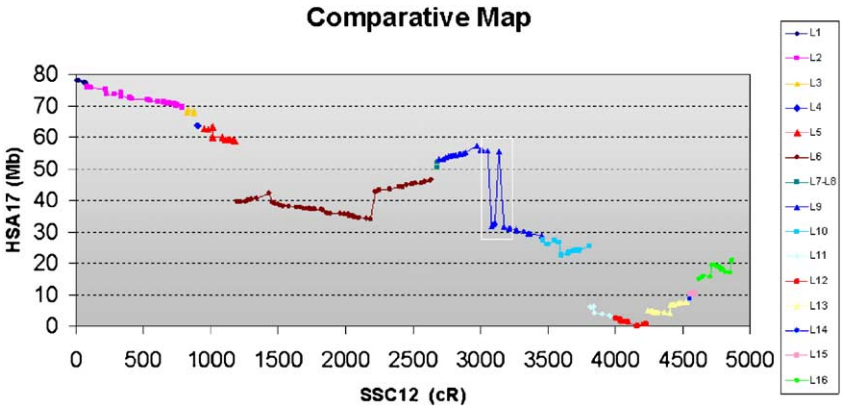

Fig. 2. Comparison of gene order between SSC12 and HSA17. A total of 245 genes (ESTs) were compared based on their positions on HSA17 and on SSC12. The positions of genes on HSA17 (human genome sequence, Build 35.1) are compared with the positions of the corresponding genes on the SSC12 $RH_{12,000\text{-rad}}$ map (Fig. 1). Map distances (cR) for SSC12 are the accumulated sum of the linkage groups (L1–L16) from Fig. 1 (Supplementary Table 1). Each dot represents a gene and its Cartesian coordinates. Each color designates a different linkage group. An abrupt change in coordinates between adjacent genes indicates a rearrangement. Individual linkage groups (L1 to L16) on the SSC12 $RH_{12,000\text{-rad}}$ map are highlighted and denoted on the right side. The gene rearrangement in the box (L9) is discussed in detail in the text.

genome sequence (Build 35.1), we could determine the distances between paired markers for four genes: *AP2B1* and *AR040A05*, 136.5 kb; *SMAECE1* and *AR054E08*, 11.9 kb; *STAT5A* and *AR060G08*, 3.4 kb; and *TOP2A* and *AR077C06*, 11.7 kb. These intervals corresponded to 12.4, 4.8, 2.5, and 12.8 $cR_{12,000}$, respectively, in the current SSC12 RH map. These data suggest that the 12,000-rad IMNpRH2 panel provides a high-resolution scaffold for interval mapping and sequencing of the swine genome.

Comparative map

To construct a comparative map of the pig and human genomes we first determined the positions in the human genome sequence (Build 35.1) for ESTs/genes mapped on the SSC12 $RH_{12,000\text{-rad}}$ panel (Fig. 1, Supplementary Table 1). We found that all 202 orthologs on HSA17 mapped on SSC12. Of 98 swine ESTs mapped, 63 matched an annotated sequence on HSA17. The remaining 35 ESTs ordered on SSC12 did not show significant similarity to any sequence in the human genome (Build 35.1) (Fig. 1, Supplementary Table 1). Among the 63 ESTs that had orthologs on HSA17, 52 were annotated. The corresponding human genes are shown in Fig. 1 (also in Supplementary Table 1) with their EST designation in parentheses. The remaining 11 ESTs did not match to any human coding sequence on HSA17. This observation provides initial molecular support for bidirectional chromosome painting results [19–21] suggesting that SSC12 and HSA17 are significantly conserved. However, when gene order was compared between the two species, six distinct macro-rearrangements (colored arrows in Fig. 1) were identified. When we analyzed the coordinates of 245 genes (ESTs) based on their position on HSA17 and SSC12 (Fig. 2), we observed that within the apparent complete synteny between HSA17 and SSC12 there are two major intrachromosomal inversions (Fig. 2). The first inversion occurs in the regions of 34.1–42.4 Mb (*MLLT6–RPIP8*) and 43.0–57.4 Mb (*NPEPPS–APPBP2*) on HSA17, while the second inversion occurs in the distal region on HSA17p (or SSC12q) that corresponds to 0.0–6.3 Mb (*ABR–FLJ10156*) and 4.5–21.0 Mb (*ALOX15–PMI*) on HSA17. We also observed micro-rearrangements within the synteny segments, particularly in the larger linkage groups (Fig. 2). For example, sequence blocks of ~2.8 Mb (39.6–42.4 Mb on HSA17) in L6, ~2.8 Mb (22.7–25.5 Mb) in L10, ~0.8 Mb (4.5–5.3 Mb) in L13, and ~2.5 Mb (17.1–19.6 Mb) in L16 are apparently inverted (Fig. 2). In L9, there were at least two subgroups of genes; one subgroup locates between 53.3 and 57.4 Mb on HSA17 and the other between 28.8 and 33.0 Mb. Genes adjacent to the boundary of the two subgroups within ~2 Mb have also gone through a series of rearrangements (boxed genes in Fig. 2).

Discussion

The 12,000-rad IMNpRH2 panel complements the 7000-rad IMpRH panel and provides a 2–3× higher resolution across the porcine genome ([16] and this study). The IMNpRH2 panel has been used successfully to construct high-resolution maps for the RN (RN locus) region on SSC15q25 [16], a QTL region on SSC7q11–q14 [18], and a region on SSC6q1.2 [17]. It has not been used to construct a map for an entire chromosome. This is the first attempt to use the panel to construct a high-resolution RH map for an entire chromosome. The SSC12 $RH_{12,000\text{-rad}}$ map contains 320 markers and covers ~4836.9 cR. We observed ~2.2-fold increase in resolution over the SSC12 $RH_{7000\text{-rad}}$ map (http://www.ag.unr.edu/beattie/research.htm), slightly less than the 2.4-, 2.8-, and 3.0-fold increases in resolution observed in regions on SSC7q11–q14 [18], SSC15q25 [16], and SSC6q1.2 [17], respectively. We estimate the average resolution of the IMNpRH2 panel at ~15.3 kb/$cR_{12,000}$, also relatively lower than the 12–14, 10.7, and 6.6 kb/$cR_{12,000}$ observed in the SSC15q25 [16], SSC7q11–q14 [18], and SSC6q1.2 regions [17]. We propose that, first, previous studies with the IMNpRH2 panel all focused on a small region

of the porcine genome, e.g., 2.4 Mb on SSC15q25 [16], 5 Mb on SSC7q11–q14 [18], and 1.4 Mb on SSC6q1.2 [17]. None of these regions contain a centromere. Although the resolution estimated from these small regions demonstrates the potential mapping power of the IMNpRH2 panel, it should probably not be applied to an entire chromosome or the whole genome when centromeric and long stretches of repeat sequences are taken into account. In addition, the fact that the kb/cR ratio was not constant and variations in the regions characterized by Yerle et al. [16] may explain the difference in mapping resolution among different regions of the genome. Second, the marker density on SSC12 was 1 marker per ~252 kb (74 Mb/294 effective positions), in comparison to ~133 (2.4 Mb/18) and ~68 kb (1.37 Mb/20) in the region of SSC15q25 [16] and SSC6q1.2 [17], respectively. The relatively low marker density on SSC12 could also play a role in the lower estimate of the kb/cR ratio.

One of the best ways to test map resolution is to design more than one pair of primers from different regions of a given gene and then map them on the same RH panel. The expected outcome of the test would be that paired markers map to the same location or adjacent to each other depending on the physical distance between the two markers. In the present study, we analyzed nine paired markers designed from nine genes across SSC12. We found that all paired markers mapped either to the same position or next to each other over a short distance, indicating the high resolution and reliability of the IMNpRH2 panel.

The order of the 16 linkage groups was based on the order of MS markers on the SSC12 genetic map (Fig. 1). Several MSs were included in the larger linkage groups such as L2, L6, and L9. The order of these MSs in their corresponding group on the SSC12 $RH_{12,000\text{-rad}}$ map is in complete agreement with their order on the genetic map (Fig. 1). After comparing the SSC12 $RH_{12,000\text{-rad}}$ map with the second-generation EST map built on the $IMpRH_{7000\text{-rad}}$ panel (http://www.ag.unr.edu/beattie/research.htm), we identified a total of 99 markers including 10 MSs and 89 ESTs common to both RH maps. In general, the two maps are in agreement and support each other. The orders for the 10 common MSs are identical in both maps. However, the order of the 89 common EST markers is not identical between the $RH_{7000\text{-rad}}$ and the $RH_{12,000\text{-rad}}$ maps. We observed several instances of marker flip (data not shown) between the two maps. These flips usually involved two to six markers in a narrow region. Recently, a high-resolution SSC12 $RH_{7000\text{-rad}}$ map of 205 genes with 2 linkage groups at LOD 6.0 was developed using the IMpRH panel (T. Shimogiri et al., submitted for publication). A significant number of the mapped genes (189/205; 92.2%) are in common with our 12,000-rad RH map. The linkage groups L1–L13 and L15 and L16 on our map correspond to linkage groups 1 and 2 in the Shimogiri et al. (submitted for publication) 7000-rad map, respectively, in identical order, while markers in L14 were not mapped on the 7000-rad map. When the order of the 189 genes was compared between the two maps, we also observed several instances of marker flip (data not shown). This finding is not unexpected as every marker was flipped internally to improve order when the maps were constructed. It is worth noting that, when we compared the gene order between SSC12 and HSA17, we identified only a few gene rearrangements within narrow regions except for the major break points of the intrachromosomal inversions (Fig. 2). Therefore, we believe that the SSC12 $RH_{12,000\text{-rad}}$ map is more accurate and reliable based on the positions of paired markers from 9 genes and from a comparison of the gene order of 245 genes (ESTs) between SSC12 and HSA17 (Fig. 2).

It is believed that each chromosome is the product of evolution, shaped by processes that have arranged and exchanged sequences, and has provided the basis for a range of genetically determined and genomically influenced traits [46]. Comparative mapping and bidirectional Zoo-FISH between mammalian species have demonstrated that HSA17 is one of the largest continuing segments in the mammalian ancestor [47] and is conserved entirely within a single chromosome in many mammalian species, including SSC12 in swine [19–21], BTA19 in cattle [48–50], OAR11 in sheep [51], ECA11 in horse [52], and FCA E1 in cat [53]. However, in mouse and rat, although the entire HSA17 appears conserved within MMU11 and RNO10, MMU11 and RNO10 also share homology with several other human chromosomes [54]. Extensive efforts to compare the gene order between SSC12 and HSA17 were first made by Shi et al. [41] and Rink et al. [11]. However, no definitive correlation could be developed because of the limited number of EST/gene markers. The RH map presented in this study overcomes this limitation and facilitates comparison of the detailed gene order between SSC12 and HSA17. It also provides an opportunity to integrate the RH and cytogenetic maps and confirm previous FISH mapping results. The porcine clathrin heavy polypeptide (*CLTC*) gene previously mapped to SSC 2p16–p17 by FISH [55] was considered the homolog of the human *CLTC* on HSA17 by in silico comparative mapping [56]. However, porcine *CLTC* mapped to SSC12 in the present study (Fig. 1) and a study using the $IMpRH_{7000\text{-rad}}$ panel (T. Shimogiri et al., submitted for publication). Most importantly, we found that the synteny group of *YPEL2–CLTC–TUBD1–RPS6KB1* on SSC12 is completely conserved on HSA17. As this work focused on a single chromosome, rather than the entire genome, we cannot exclude the possibility of a second copy of the *CLTC* gene in the porcine genome, as a *CLTCL* (*CTLC*-like1) mapped to HSA22 in the human genome [57].

Among 245 human orthologs analyzed [18.1% (245/1354) of the total number of genes on HSA17], none mapped to a porcine chromosome other than SSC12. Thus, we conclude that SSC12 and HSA17 appear completely conserved. However, coordinate analysis of these genes on HSA17 and SSC12 identifies intrachromosomal rearrangements between the highly conserved chromosomes occurring at two levels: macro and micro. Macro-rearrangements were identified as six large synteny blocks (Fig. 1), four of which were in an inverted orientation (Figs. 1 and 2). Two major inversions from the short-arm telomeric region to the middle of SSC12 and in the distal region of SSC12q were detected. The relatively high resolution of the

SSC12 $RH_{12,000}$ map allowed us to detect several small (0.8 to 2.8 Mb on HSA17) inverted regions compared with the human genome sequence. In addition, it also allowed us to explore the process of rearrangement during the evolution of SSC12. If we take linkage group 9 as an example, we think the current order of genes, *PS6KB1–THRAP1–BCA33–PPM1D–APPBP2–TRIP3–LHX1–ACACA–AP1GBP1–ABC1–CCT4L1* (within the box in Figs. 1 and 2), is a consequence of a series of inversions that occurred within an ~3.2-Mb region (Supplementary Table 1). The first event happened when the segment (55.5–57.4 Mb on HSA17) containing genes *ABC1–APPBP2–PPM1D–BCA33–THRAP1* was inverted, and then one end (*ABC1* end at position 55.5 Mb) of the segment joined with another segment (28.8–33.0 Mb on HSA17) containing *AP1GBP1–ACACA–LHX1–TRIP3–CCT4L1* at position 33.0 Mb on HSA17 (Fig. 2), producing a boundary between *ABC1* and *AP1GBP1* on SSC12. The next inversion involved genes adjacent to the boundary, including gene *ABC1* (position 55.5 Mb on HSA17) on one side of the boundary and *AP1GBP1–ACACA–LHX1–TRIP3* (31.9–33.0 Mb on HSA17) on the other side, and the original order of *APPBP2–ABC1–AP1GBP1–ACACA–LHX1–TRIP3–CCT4L1* was inverted into *APPBP2–TRIP3–LHX1–ACACA–AP1GBP1–ABC1–CCT4L1*. Results from this study support a previous finding that chromosomal inversion is one of the two dominant factors (the other factor is translocation) in chromosomal evolution in mammals [58].

Markers in the centromeric regions of chromosomes often show the highest retention frequencies. This so-called "centromeric effect" was observed in several species, including human [59,60], cattle [61], and chicken [62,63]. In the present study, we observed that markers in two regions of SSC12 have significantly higher RF in comparison with markers in the rest of the chromosome (Supplementary Table 1). One region is around the centromere of SSC12 and the other is located on SSC12q between S0147 and TIAF1, corresponding to the centromere of HSA17 (Fig. 1). This finding not only indicates a centromeric effect on SSC12, but also suggests a transmitting centromeric effect from HSA17 (or the corresponding chromosome from the mammalian ancestor) to SSC12 during the course of evolution. To our knowledge, transmitting centromeric effect from one species to another has never been reported in the literature. It would be interesting to see whether this kind of effect is a common phenomenon in mammals. We also observed a region on SSC12q between *ALOX12* and *P101-P13K* with significantly lower RFs (Fig. 1, Supplementary Table 1), indicating that this particular region of SSC12 is underrepresented in the IMNpRH2 panel. Within this region, we found that the order of three ESTs/genes of two groups [*AR056G04–ACADVL–HSA011916* and *MPDU1–FXR2–EIF4A1* (L13)] could not be resolved because of the identical RH vector of the markers, suggesting that the lower RF had a negative effect on map resolution in this region of the RH map.

In summary, these data represent the largest single assignment of type I markers to an RH map of SSC12, providing the highest resolution for any physical or EST map of a porcine chromosome to date. The data support previous Zoo-FISH results [19–21] at the molecular level and demonstrate that SSC12 and HSA17 are highly conserved although intrachromosomal macro- and micro-rearrangements occur. The current $RH_{12,000\text{-rad}}$ map of SSC12 and the IMNpRH2 panel will be useful in establishing a scaffold for sequencing the swine genome and fine-mapping the QTL reported on SSC12 and other chromosomes.

Materials and methods

Genes, ESTs, and microsatellite markers

Of the 208 genes analyzed, 194 genes were isolated from a normalized cDNA library constructed from the porcine olfactory bulb as described by Fujisaki et al. [64] and selected as orthologs to well-annotated HSA17 genes (*e* values $\leq 10^{-100}$) (T. Shimogiri et al., submitted for publication). The remaining 14 genes were collected from the literature (Supplementary Table 1). A total of 103 EST markers were derived from a panel of normalized porcine cDNA libraries as described earlier [11,65]. Primers were designed to amplify putative exons of the selected porcine ESTs/genes with PRIMER3 (http://frodo.wi.mit.edu/cgi-bin/primer3/primer3_www.cgi) [66]. All primers were optimized by determining the highest annealing temperature at which successful amplification of porcine genomic DNA took place. Primers were then tested with porcine and Chinese hamster genomic DNA at that temperature for species specificity. Primer sequences for the 26 microsatellites were obtained from the literature (http://www.marc.usda.gov/genome/genome.html).

During the course of this study, we avoided designing redundant primer pairs for a given gene or EST. However, we still identified nine genes with two pairs of primers synthesized (one pair designed from the gene cDNA sequence and synthesized in Japan and the other pair from the corresponding EST, synthesized in the United States). We decided to treat the two pairs of primers as two individual markers and typed them separately with the IMNpRH2 panel. We reasoned that map results from the redundant primer pairs would serve as internal controls to evaluate mapping accuracy and resolution of the IMNpRH2 panel.

RH typing

A 12,000-rad IMNpRH2 panel [16] containing 90 hybrids was used in this study. All PCR typing reactions were performed in 96-well Techne Touchgene thermocyclers. Each PCR contained 25 ng of hybrid DNA, 1× PCR buffer (Bioline, MA, USA), 0.4 μM each primer, 1.5 mM $MgCl_2$, 66 μM each dNTP, 1× cresol loading dye [67], and 0.3 U of Immolase DNA polymerase in a total volume of 15 μl. The amplification cycle included an initial 95°C, 7-min denaturing step, followed by cycling between 94°C for 15 s, 57–69°C for 30 s, and 72°C for 30 s, and a final extension step at 72°C for 5 min. Controls consisted of porcine and hamster genomic DNA and a reaction containing no DNA. The first PCR was routinely run for 40 cycles and the second PCR for between 33 and 40 cycles depending on the level of background amplification and intensity of pig-specific bands. If more than four discrepancies were observed between the first and the second PCR, a third PCR was carried out. The PCR products were electrophoresed on 2% agarose gels, visualized, and photographed with an AlphaImager 2200 (Alpha Innotech Corp., San Leandro, CA, USA). At least two gel images per marker were independently scored by two individuals using GelScore (http://www.weswbarries.com/GelScore/). Consensus vectors were established by two individuals using GelScore data as a baseline. Markers with unusually high or low retention frequencies or with more than four discrepancies were eliminated. Markers were scored as present (1), absent (0), or ambiguous (2).

Construction of the SSC12 $RH_{12,000}$ map

Markers were ordered and the map was constructed with CarthaGene software [43,44]. Marker consensus vectors were loaded into the program and grouped together at LOD 6.0 and a maximum distance of 100 cR between markers. This gave the program a base map to utilize for all further

analysis. While the build framework (*buildfw*) command is often used to generate reliable maps, it is also a method that generates incomplete maps. A marker can be added to the map only if the difference in log-likelihood between the best and the second best position is greater than a user-defined threshold. The process stops when no marker with sufficient quality exists. This can lead to a situation in which some markers must be forced into position so that the map will contain all markers. To avoid a situation in which marker orders would be forced, each linkage group was analyzed using a simulated annealing. Simulated annealing exploits an analogy with metallurgy/thermodynamics. When a physical system is at a high temperature, the atoms in the system are in a highly disordered state. Lowering the temperature of the system results in the atoms of the system acquiring a more orderly state. The simulation initiated at 300°C and worked down to 0.1°C. At each temperature, the simulated annealing was repeated 100 times. After each iteration, the temperature was reduced by 20% and the process repeated. Any improvements to the best ordered map were put into the heap (resident memory) as the new best map. After the annealing was completed, the best ordered map for that linkage group was subjected to an improving method in which each marker was flipped internally to try to better the final map order. A window size of at least four markers was applied, with the largest linkage groups using a window size of either six or eight markers. The best map was compared (order-wise) to the genetic map and the $RH_{7000\text{-}rad}$ map to verify marker order. Maps were drawn using MapCreator (http://www.wesbarris.com/mapcreator/).

Comparative mapping

All sequences of the porcine ESTs were BLAT searched against the human genome sequence (Build 35.1) (http://genome.ucsc.edu/cgi-bin/hgBlat?command = start), which allowed us to find quickly sequences of 95% and greater similarity of length 40 bases or more. Once a sequence match was identified, the start position of the sequence in the human genome was collected (Fig. 1, Supplementary Table 1). Chromosomal locations and start positions of their orthologs in the human genome were also established for all porcine genes analyzed (Supplementary Table 1, Fig. 1) using the NCBI human Map Viewer (Build 35.1) (http://www.ncbi.nlm.nih.gov/mapview/). Cartesian coordinates of 245 genes (ESTs) based on their map positions on HSA17 and on SSC12 were also developed (Fig. 2). Map distances (cR) for SSC12 in Fig. 2 were the accumulated sums of the linkage groups (L1–L16) from Fig. 1.

Acknowledgments

This work was supported by a grant from the USDA-CSREES (2004-35205-14244) to C.W.B. and the Program for the Promotion of Basic Research Activity for Innovative Biosciences of the Bio-oriented Technology Research Advancement Institution, Japan (H.Y.). It was also supported in part by the Nevada Agricultural Experiment Station, Publication No. 53055520.

Appendix A. Supplementary data

Supplementary data associated with this article can be found in the online version at doi:10.1016/j.ygeno.2005.07.007.

References

[1] D.R. Cox, M. Burmeister, E.R. Price, S. Kim, R.M. Myers, Radiation hybrid mapping: a somatic cell genetic method for constructing high-resolution maps of mammalian chromosomes, Science 250 (1990) 245–250.

[2] A.P. Rattink, M. Faivre, B.J. Jungerius, M.A. Groenen, B. Harlizius, A high-resolution comparative RH map of porcine chromosome (SSC) 2, Mamm. Genome 12 (2001) 366–370.

[3] H. Cao, et al., A high-resolution radiation hybrid map of porcine chromosome 6, Anim. Genet. 35 (2004) 367–378.

[4] S.A. McCoard, et al., An integrated comparative map of the porcine X chromosome, Anim. Genet. 33 (2002) 178–185.

[5] N. Hamasima, et al., Construction of a new porcine whole-genome framework map using a radiation hybrid panel, Anim. Genet. 34 (2003) 216–220.

[6] A. Mikawa, et al., Characterization of 298 ESTs from porcine back fat tissue and their assignment to the SSRH radiation hybrid map, Mamm. Genome 15 (2004) 315–322.

[7] M. Yerle, et al., Construction of a whole-genome radiation hybrid panel for high-resolution gene mapping in pigs, Cytogenet. Cell Genet. 82 (1998) 182–188.

[8] R.J. Hawken, et al., A first-generation porcine whole-genome radiation hybrid map, Mamm. Genome 10 (1999) 824–830.

[9] D. Milan, et al., IMpRH server: an RH mapping server available on the Web, Bioinformatics 16 (2000) 558–559.

[10] N. Sarker, et al., Directed isolation and mapping of microsatellites from swine chromosome 1q telomeric region through microdissection and RH mapping, Mamm. Genome 12 (2001) 524–527.

[11] A. Rink, et al., A first-generation EST RH comparative map of the porcine and human genome, Mamm. Genome 13 (2002) 578–587.

[12] R. Middleton, J. Aldenhoven, Y. Chen, B. Backofen, C. Moran, Improving the comparative map of porcine chromosome 9 with respect to human chromosomes 1, 7 and 11, Cytogenet. Genome Res. 102 (2003) 128–132.

[13] M. Van Poucke, et al., A refined comparative map between porcine chromosome 13 and human chromosome 3, Cytogenet. Genome Res. 102 (2003) 133–138.

[14] S.N. Meyers, et al., Construction of a high-resolution physically-anchored human–pig comparative WG–RH map, PAG-XII abstracts (2004) 671.

[15] Y. Lahbib-Mansais, et al., Contribution to high-resolution mapping in pigs with 101 type I markers and progress in comparative map between humans and pigs, Mamm. Genome 14 (2003) 275–288.

[16] M. Yerle, et al., Generation and characterization of a 12,000-rad radiation hybrid panel for fine mapping in pig, Cytogenet. Genome Res. 97 (2002) 219–228.

[17] F. Martins-Wess, et al., A high-resolution physical and RH map of pig chromosome 6q1.2 and comparative analysis with human chromosome 19q13.1, BMC Genom. 4 (2003) 20.

[18] O. Demeure, et al., Rearranged gene order between pig and human in a QTL region on SSC 7, Mamm. Genome 14 (2003) 71–80.

[19] G. Rettenberger, et al., Visualization of the conservation of synteny between humans and pigs by heterologous chromosomal painting, Genomics 26 (1995) 372–378.

[20] L. Frönicke, B.P. Chowdhary, H. Scherthan, I. Gustavsson, A comparative map of the porcine and human genomes demonstrates ZOO-FISH and mapping-based chromosomal homologies, Mamm. Genome 7 (1996) 285–290.

[21] A. Goureau, et al., Human and porcine correspondence of chromosome segments using bidirectional chromosomal painting, Genomics 36 (1996) 252–262.

[22] E. Casas-Carrillo, A. Prill-Adams, S.G. Price, A.C. Clutter, B.W. Kirkpatrick, Mapping genomic regions associated with growth rate in pigs, J. Anim. Sci. 75 (1997) 2047–2053.

[23] S.A. Knott, et al., Multiple marker mapping of quantitative trait loci in a cross between outbred wild boar and large white pigs, Genetics 149 (1998) 1069–1080.

[24] G.A. Rohrer, Identification of quantitative trait loci affecting birth characters and accumulation of backfat and weight in a Meishan(White Composite resource population, J. Anim. Sci. 78 (2000) 2547–2553.

[25] D.J. de Koning, et al., Detection and characterization of quantitative trait loci for growth and reproduction traits in pigs, Livest. Prod. 72 (2001) 185–198.

[26] L. Andersson-Eklund, et al., Mapping quantitative trait loci for carcass and meat quality traits in a wild boar × Large White intercross, J. Anim. Sci. 76 (1998) 694–700.

[27] M. Malek, et al., A molecular genome scan analysis to identify

chromosomal regions influencing economic traits in the pig: II. Meat and muscle composition, Mamm. Genome 12 (2001) 637–645.
[28] A.A. Paszek, et al., Interval mapping of carcass and meat quality traits in a divergent swine cross, Anim. Biotechnol. 12 (2001) 155–165.
[29] D. Milan, et al., Detection of quantitative trait loci for carcass composition traits in pigs, Genet. Sel. Evol. 34 (2002) 705–728.
[30] A. Clop, et al., Detection of QTL affecting fatty acid composition in the pig, Mamm. Genome 14 (2003) 650–656.
[31] J.P. Cassady, et al., Identification of quantitative trait loci affecting reproduction in pigs, J. Anim. Sci. 79 (2001) 623–633.
[32] H. Hirooka, et al., A whole-genome scan for quantitative trait loci affecting teat number in pigs, J. Anim. Sci. 79 (2001) 2320–2326.
[33] I. Edfors-Lilja, E. Wattrang, L. Andersson, C. Fossum, Mapping quantitative trait loci for stress induced alterations in porcine leukocyte numbers and functions, Anim. Genet. 31 (2000) 186–193.
[34] H. Ellegren, et al., A primary linkage map of the porcine genome reveals a low rate of genetic recombination, Genetics 137 (1994) 1089–1100.
[35] G.A. Rohrer, L.J. Alexander, J.W. Keele, T.P. Smith, C.W. Beattie, A microsatellite linkage map of the porcine genome, Genetics 136 (1994) 231–245.
[36] A.L. Archibald, et al., The PiGMaP Consortium linkage map of the pig (Sus scrofa), Mamm. Genome 6 (1995) 157–175.
[37] G. Rettenberger, et al., Chromosomal assignment of seventeen porcine microsatellites and genes by use of a somatic cell hybrid mapping panel, Anim. Genet. 26 (1995) 269–273.
[38] M. Yerle, Y. Lahbib-Mansais, P.D. Thomsen, J. Gellin, Localization of the porcine growth hormone gene to chromosome 12p1.2 → p1.5, Anim. Genet. 24 (1993) 129–131.
[39] R. Davoli, et al., Isolation of porcine expressed sequence tags for the construction of a first genomic transcript map of the skeletal muscle in pig, Anim. Genet. 3 (2002) 3–18.
[40] J. Yang, et al., Assignments of GRB7, GCN5L2, COL1A1 and TBCD to pig chromosome 12 by radiation hybrid mapping, Cytogenet. Genome Res. 103 (2003) 204L.
[41] X.W. Shi, et al., Radiation hybrid comparative mapping between human chromosome 17 and porcine chromosome 12 demonstrates conservation of gene order, Anim. Genet. 32 (2001) 205–209.
[42] A. Robic, et al., A new contribution to the integration of human and porcine genome maps: 623 new points of homology, Cytogenet. Genome Res. 102 (2003) 100–108.
[43] T. Schiex, C. Gaspin, CARTHAGENE: constructing and joining maximum likelihood genetic maps, Proc. Int. Conf. Intell. Syst. Mol. Biol. 5 (1997) 258–267.
[44] T. Schiex, P. Chabrier, M. Bouchez, D. Milan, Boosting EM for radiation hybrid and genetic mapping, Proceedings of the Workshop on Algorithms in Bioinformatics, 2001, pp. 41–50.
[45] Schmitz, et al., Swine chromosomal DNA quantification by bivariate flow karyotyping and karyotype interpretation, Cytometry 13 (1992) 703–710.
[46] H.F. Willard, Tales of the Y chromosome, Nature 423 (2003) 810–813.
[47] L.W. Hillier, et al., Sequence and comparative analysis of the chicken genome provide unique perspectives on vertebrate evolution, Nature 432 (2004) 695–716.
[48] S. Solinas-Toldo, C. Lengauer, R. Fries, Comparative genome map of human and cattle, Genomics 27 (1995) 489–496.
[49] Y.P. Yang, C.E. Rexroad III, J. Schlapfer, J.E. Womack, An integrated radiation hybrid map of bovine chromosome 19 and ordered comparative mapping with human chromosome 17, Genomics 48 (1998) 93–99.
[50] M.R. Band, et al., An ordered comparative map of the cattle and human genomes, Genome Res. 10 (2000) 1359–1368.
[51] B.P. Chowdhary, L. Frönicke, I. Gustavsson, H. Scherthan, Comparative analysis of the cattle and human genomes: detection of ZOO-FISH and gene mapping-based chromosomal homologies, Mamm. Genome 7 (1996) 297–302.
[52] T. Raudsepp, L. Fronicke, H. Scherthan, I. Gustavsson, B.P. Chowdhary, Zoo-FISH delineates conserved chromosomal segments in horse and man, Chromosome Res. 4 (1996) 218–225.
[53] F. Yang, et al., Reciprocal chromosome painting illuminates the history of genome evolution of the domestic cat, dog and human, Chromosome Res. 8 (2000) 393–404.
[54] G. Bourque, P.A. Pevzner, G. Tesler, Reconstructing the genomic architecture of ancestral mammals: lessons from human, mouse, and rat genomes, Genome Res. 14 (2004) 507–516.
[55] P.D. Thomsen, A.K. Wintero, M. Fredholm, Chromosomal assignments of 19 porcine cDNA sequences by FISH, Mamm. Genome 9 (1998) 394–396.
[56] Z. Jiang, et al., Measuring conservation of contiguous sets of autosomal markers on bovine and porcine genomes in relation to the map of the human genome, Genome 45 (2002) 769–776.
[57] K.R. Long, et al., Cloning and characterization of a novel human clathrin heavy chain gene (CLTCL), Genomics 35 (1996) 466–472.
[58] W.J. Murphy, G. Bourque, G. Tesler, P. Pevzner, S.J. O'Brien, Reconstructing the genomic architecture of mammalian ancestors using multispecies comparative maps, Hum. Genom. 1 (2003) 30–40.
[59] G. Gyapay, et al., A radiation hybrid map of the human genome, Hum. Mol. Genet. 5 (1996) 339–346.
[60] E.A. Stewart, et al., An STS-based radiation hybrid map of the human genome, Genome Res. 7 (1997) 422–433.
[61] E. Kurar, J.E. Womack, B.W. Kirkpatrick, A radiation hybrid map of bovine chromosome 24 and comparative mapping with human chromosome 18, Anim. Genet. 34 (2003) 198–204.
[62] F. Pitel, et al., A high-resolution radiation hybrid map of chicken chromosome 5 and comparison with human chromosomes, BMC Genom. 5 (2004) 66.
[63] T.S.K.M. Rabie, et al., A radiation hybrid map of chicken chromosome 4, Mamm. Genome 15 (2004) 560–569.
[64] S. Fujisaki, et al., Analysis of a full-length cDNA library constructed from swine olfactory bulb for elucidation of expressed genes and their transcription initiation sites, J. Vet. Med. Sci. 66 (2004) 15–23.
[65] A. Rink, E.M. Santschi, C.W. Beattie, Normalized cDNA libraries from a porcine model of orthopedic implant-associated infection, Mamm. Genome 13 (2002) 198–205.
[66] S. Rozen, H.J. Skaletsky, Primer3 on the WWW for general users and for biologist programmers, Methods Mol. Biol. 132 (2000) 365–386.
[67] E. Hodges, S.M. Boddy, S. Thomas, J.L. Smith, Modification of IgH PCR clonal analysis by the addition of sucrose and cresol red directly to PCR reaction mixes, Mol. Pathol. 50 (1997) 164–166.